Copyright 2024 by Mr. Vassilios Silaidis. Published by the IAF, with permission and released to the IAF to publish in all forms .

IAC-24-B6, IP, 25, x84181

Multi-Disciplinary Optimization of Air-Launched Vehicles: A Genetic Algorithm Approach

Vassilios Silaidis[a]*, Stefania Carlotti[b], Alberto Carboni[d], Filippo Maggi[c]

[a]PhD Student, Aerospace Science and Technology Dept., Politecnico di Milano, Via La Masa 34, Milano 20156, Italy vassilios.silaidis@polimi.it
[b]Researcher, Aerospace Science and Technology Dept., Politecnico di Milano, Via La Masa 34, Milano 20156, Italy, stefania.carlotti@polimi.it,AIAA Member
[c]Associate Professor, Aerospace Science and Technology Dept., Politecnico di Milano, Via La Masa 34, Milano 20156, Italy, filippo.maggi@polimi.it, Senior AIAA Member
[d]Future Systems, MBDA Italia, Via Monte Flavio, Roma 00131, Italy alberto.carboni@mbda.it
*Corresponding Author

Abstract

Air-launched vehicles play a crucial role in space exploration and satellite deployment, offering unique advantages such as flexibility in launch location and trajectory optimization. However, designing these vehicles involves complex trade-offs among aerodynamics, propulsion, and trajectory dynamics, necessitating sophisticated optimization techniques. This article presents a comprehensive framework for the multi-disciplinary analysis and optimization of air-launched vehicles, leveraging a genetic algorithm (GA) to optimize the main mission subsystems. Aerodynamic evaluations are conducted using a fast aerodynamic-predictive model, which relies on the geometrical parameters of the system. Propulsion performance parameters, obtained via Chemical Equilibrium with Applications (CEA), are optimized to satisfy constraints on thrust-to-weight ratio and dimensional requirements. Additionally, trajectory dynamics are governed by a pitch and yaw history guidance system. The study aims to maximize the performance - i.e. minimizing the global lift-off mass or minimizing the production cost of a preliminary-designed air-launch vehicle. Critical constraints related to either system's parameters (i.e. stability, robustness of proposed candidates), and mission parameters (i.e. target orbit, mission phases) will be enforced to ensure the feasibility and safety of the optimized configurations.

Keywords: air-launched vehicles, genetic algorithms, launch systems, rocket propulsion, launcher aerodynamics, system optimization

Nomenclature

A_e	engine exit area [m^2]
A_t	engine throat area [m^2]
A_{wet}	wing surface wetted by the airflow [m^2]
b_t	tail surface span [m]
b_w	wing surface span [m]
C_{A_W}	axial coefficient due to wave interference
$C_{A_{S_F}}$	axial coefficient due to skin friction
C_{A_B}	axial coefficient due to base body interference
C_{d_n}	crossflow drag coefficient
C_L	lift coefficient
C_{L_α}	lift slope coefficient
C_D	drag coefficient
$C_{N_{NKP}}$	normal coefficient according to NKP theory
C_{N_0}	C_N of a circular reference body
C^*	characteristic velocity
C_T	thrust coefficient
$C_{f\infty}$	free-stream turbulent skin friction coefficient
cr_t	tail surface root chord [m]
cr_w	wing root chord [m]
$\vec{D}$	drag force [N]
d	body diameter [m]
$\vec{F_g}$	gravitational force [N]
g_0	gravitational acceleration [m/s^2]
h_0	launch altitude [m]
I_{sp}	specific impulse [s]
$\vec{L}$	lift force [N]
l	length of the body [m]
lat_0	launch latitude [deg]
lon_0	launch longitude [deg]
l_n	length of the nose [m]
l_t	distance from nose tip to tail surface [m]
l_w	distance from nose tip to wing surface [m]
M	Mach number
M_∞	free stream Mach number
m	mass of the body [kg]
m_0	initial mass at launch [kg]
n_t	nose type geometry
$\vec{n}$	versor perpendicular to velocity vector
P_a	ambient pressure [Pa]
q	dynamic pressure [Pa]
$\vec{r}$	position vector
Re	Reynold number
R_e	Earth radius [m]

Copyright 2024 by Mr. Vassilios Silaidis. Published by the IAF, with permission and released to the IAF to publish in all forms .

S_{ref}	reference surface of the body
t_{mac}	thickness of the wing
t_b	burning time [s]
$\vec{T}$	thrust engine force [N]
T_{vac}	Vacuum thrust [-]
$\hat{u}$	thrust engine direction vector
u_e	exit velocity [m/s]
$\vec{v}$	velocity vector in ECI system
v_0	launch velocity [m/s]
$\overrightarrow{v_{in}}$	inertial velocity [m/s]
$\overrightarrow{v_{LV}}$	launcher vehicle velocity at launch [m/s]
$\overrightarrow{v_{rel}}$	relative velocity [m/s]
$\overrightarrow{v_w}$	wind velocity [m/s]
w	weights of the objective function
α	angle of attack [deg]
γ	specific heat ratio of air
γ_0	launch flight path angle [deg]
η	crossflow drag factor
μ_e	Earth gravitational constant $[m^3/s^{-2}]$
θ	pitch angle [deg]
ψ	yaw angle [deg]
ρ	air density [kg/m^3]
ε	motor expansion ratio
ϵ	cone half-angle [deg]
ω_e	earth rotational velocity [rad/s]

Acronyms/Abbreviations

Air-launched vehicle	(ALV)
Earth Centred Inertial	(ECI)
Genetic Algorithm	(GA)
Global Lift-off weight	(GLOW)
Mass estimation relationship	(MER)
Solid Rocket Motor	(SRM)
Three degrees of freedom	(3DOF)

1. Introduction

An Air-Launched Vehicle (ALV) is a type of rocket-propelled launch vehicle deployed from an aircraft instead of vertically launched from a traditional pad. This type of launcher offers flexibility and manoeuvrability, as it can reach orbit from different locations without needing a fixed launch site. Efficiency is also enhanced by using an aircraft as the first stage, which, other than being fully reusable, allows for launch altitudes above 10 km, reducing drag and gravity losses since the trajectory is not restricted to a vertical ascent.

However, challenges include the limitations of aircraft in terms of size, weight, and interfaces, making micro-launchers the most suitable option. Payload integration and propellant loading occur before take-off, potentially leading toissues . Despite these challenges, the approach may become more significant due to the rapid growth in the small satellite market. In fact, recent advances in electronics and miniaturization are reducing satellite mass, making these options more appealing both economically and scientifically.

Indeed, the space industry is expanding rapidly, particularly in the sector of small launchers (payloads under 200 kg) [1]. This is leading to a transition towards establishing a novel cohort of light, reusable launchers designed explicitly for the orbital injection of lightweight payloads [2] [3]. The evolution is capturing the interest of various enterprises and space agencies, driven by the objective of mitigating the expenses associated with space launches.

According to a 2021 industry survey [4] there are about 17 operational small launchers worldwide, but only two of them are air-launch capable: Pegasus by Northrop Grumman [5] and Launcher One by Virgin Orbit [6], the latter of which was cancelled due to corporate restructuring. Consequently, the industry still primarily depends on ground-based launchers.

The optimization of missions for launch vehicles has been the focus of extensive research and development for nearly half a century and research into optimization techniques is crucial in addressing these technological challenges and achieving the shared economic goals of international organizations. This paper will concentrate on optimization methods, particularly genetic algorithms (GAs) [6] [7], applied to air-launched mission scenarios, with a focus on design and performance.

Having chosen a light air-launched vehicle as baseline for the study, the aim is to optimise its geometry, propulsion and trajectory, exploiting a suitably designed framework of optimization. During optimisation it is possible to maximise several desired performance parameters simultaneously, given the multi-disciplinary nature of the method proposed. At the same time, proper constraints have been introduced to keep several others variables under control.

In the second section of this paper, genetic algorithms will be examined, providing a methodological overview and illustrating relevant applications found in the literature. The third section will delve into the simulation model employed, with particular emphasis on the development of the underlying aerodynamic and propulsion model. The fourth section will introduce the nominal case chosen as a fundamental reference for the conducted experiment. Subsequently, in the following sections, the optimization model used will be introduced, followed by the presentation of the results obtained through its application.

2. Genetic Algorithms for Aerospace Applications

The GAs represent a contemporary computing technique, named after their functional resemblance to biological and behavioural phenomena of living organisms.

The fundamental objective of a genetic algorithm search procedure is to identify and select the optimal solution to

Copyright 2024 by Mr. Vassilios Silaidis. Published by the IAF, with permission and released to the IAF to publish in all forms .

a design problemby generating a certain number of design candidates - called chromosomes - which represent solutions of the problem, and choosing among them the candidate which has the best characteristics with respect to a desired performance - called fitness - determined by an objective function. The objective function is dependent on multiple control parameters (i.e., the genes of the various chromosomes), which are typically non-linear and introduce design constraints.
The evolutionary process involves three main operations: *selection*, where fitter individuals are chosen to pass their genes to the next generation; *crossover* (or recombination), where pairs of individuals exchange parts of their chromosomes to create offspring; and *mutation*, where random changes are introduced to maintain genetic diversity and prevent premature convergence to suboptimal solutions. The procedural steps and theoretical foundations of the optimization search process can be found in the extensive literature on this topic [7][8].
Optimization in aerospace engineering applications using genetic algorithms in different disciplines have been proved with great success: examples of optimization in flight trajectories [9] [10], propulsion systems [11] [12] [13], [14], wings and airfoils [15][16], missiles [17][18], rockets [19] and aircrafts [20] [21] can be found in the literature. The significant advantages in these applications stem from the capability to integrate discrete, integer, and continuous variables, consolidating selection and sizing tasks into a unified optimization problem within conceptual design. Moreover, the use of a GA obviates the need for an initial starting point, i.e. even in the absence of a defined initial design the GA may generate output systems with optimal performance.
GA methods have also great potential to support the design of multi-disciplinary systems, as already pointed out by studies in the literature [22][20] [22].
The integration of these algorithms reduces subjective decision-making, promoting creative interaction of design features.. Their stochastic nature allows the problem to avoid getting trapped in local optima, making them especially useful where the optimization of multiple conflicting objectives (like minimizing weight while maximizing strength and aerodynamic efficiency) is analyzed. For these reasons, a multi-disciplinary feasible approach with GA has been chosen and in the next sections the details of the models used will be examined, along with the proposed architecture.

3. Modeling and Simulation

A three-dimensional point-mass model (3-DoF model) is considered for the launch vehicle [23] [24].
All the forces are represented in figure 1 acting on the body's centre of mass. The thrust is considered aligned with the body axis, the aerodynamic forces Drag and Lift follow the directions respectively aligned and perpendicular to the relative velocity vector (in Earth Centred Inertial reference frame) and the gravitational force points towards the centre of the Earth.

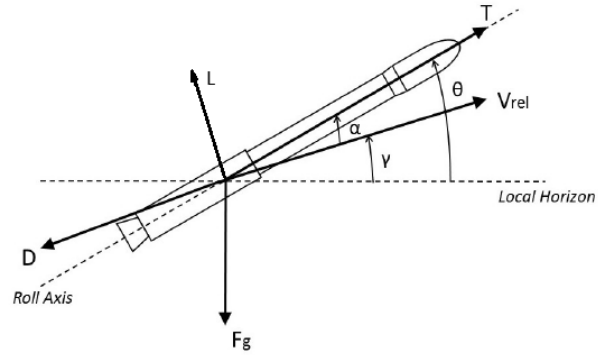

Figure 1: Forces acting on the concentrated mass of 3DOF model

The rocket state is defined by position $\vec{r}$, velocity $\vec{v}$, and mass m, the equations of motion in the inertial reference frame are listed hereafter:

$$\dot{\overrightarrow{r(t)}} = \overrightarrow{v(t)}$$

$$\dot{\overrightarrow{v(t)}} = \frac{\overrightarrow{F_g}}{m} + \frac{T(t)}{m}\hat{u}(t) + \frac{\overrightarrow{D(t)}}{m} + \frac{\overrightarrow{L(t)}}{m}$$

$$\dot{m}(t) = -\frac{T(t)}{I_{sp}g_0}$$

where the unit vector $\hat{u}(t)$ identifies the direction of the thrust T. The numerical integration is performed in the Earth Centered Inertial (ECI) reference frame. Rocket thrust, aerodynamic Drag and Lift forces and gravitational force are expressed as:

$$\vec{T} = (T_{vac} - p_a A_e)\hat{u}$$

$$\vec{D} = -\frac{1}{2}\rho_a(h)S_{ref}C_D(M,\alpha)v_{rel}^2\widehat{v_{rel}}$$

$$\vec{L} = \frac{1}{2}\rho_a(h)S_{ref}C_L(M,\alpha)v_{rel}^2\hat{n}$$

$$\vec{F_g} = -m\frac{\mu}{r^3}\vec{r} + mf_{J2}(\vec{r})$$

where the relative velocity is:

$$\overrightarrow{v_{air}} = \overrightarrow{v_{in}} - \overrightarrow{\omega_E} \times \vec{r} - \overrightarrow{v_w} \approx \overrightarrow{v_{in}} - \overrightarrow{\omega_E} \times \vec{r} = \overrightarrow{v_{rel}}$$

with the approximation of a null wind velocity.
The initial launch conditions in terms of positions and velocity are summarized hereafter:

$$\overrightarrow{r_0} = \begin{bmatrix} (R_E + h_0) * \cos(lat_0) * \cos(lon_0) \\ (R_E + h_0) * \cos(lat_0) * \sin(lon_0) \\ (R_E + h_0) * sin(lat_0) \end{bmatrix}$$

$$\overrightarrow{v_0} = \overrightarrow{v_{LV}} + \overrightarrow{v_E} = \overrightarrow{v_{LV}} + \begin{bmatrix} -\omega_E r_{y0} \\ \omega_E r_{x0} \\ 0 \end{bmatrix}$$

3.1 Aerodynamics estimation

Copyright 2024 by Mr. Vassilios Silaidis. Published by the IAF, with permission and released to the IAF to publish in all forms .

The aerodynamic prediction code is based on the methodology proposed by Jorgensen in 1977 [25] [26]. Semiempirical correlations have been used to evaluate static aerodynamic characteristics of slender body with or without lifting surfaces from null to large angles of attack. This method enables fast and low fidelity validated aerodynamic computations for preliminary studies, for a wide range of angles of attack and body shapes. The normal force coefficient for a wing-body-tail configuration is computed according to eq.(1) . , where terms representing the potential-theory crossflow and viscous-separation crossflow can be recognized.

$$C_N = C_{N_{NKP}} \frac{sin2\alpha}{2\alpha} + \frac{2\eta\, C_{d_n}}{A_r} sin^2\,\alpha \int_0^l \left(\frac{C_N}{C_{N_0}}\right)_{Newt} rdx \quad (1)$$

The potential flow contribution to C_N is computed from the linear method presented in NACA Report 1307 [27]. The reader should keep in mind that this method, referred to as the NKP method (for Nielsen, Kaattari and Pitts), is restricted to bodies of circular cross section with wings and tails that do not have swept-forward leading edges or swept-back trailing edges. As far as the axial force coefficient is concerned, for slender bodies a rough engineering estimate can be obtained with:

$$C_A = C_{A_{\alpha=0}} cos^2\alpha$$

$$C_{A_{\alpha=0}} = C_{A_W} + C_{A_{SF}} + C_{A_B}$$

where C_{A_W} represents the wave or pressure contribution from the nose or forward-facing base, $C_{A_{SF}}$is the skin-friction contribution and C_{A_B} is the base-pressure contribution [28]. For a forward-facing conical-nosed body at supersonic or hypersonic Mach numbers, the wave contribution to the total axial-force coefficient can be readily computed from the Linnell-Bailey expression:

$$C_{aw} = \frac{(4sin^2\epsilon)(2.5 + 8\beta sin\epsilon)}{(1 + 16\beta sin\epsilon)}$$

where $\beta = \sqrt{M_\infty^2 - 1}$ and ϵ is the cone half-angle.

$$C_{A_B} = -\frac{2}{\gamma M_\infty^2}\left\{\left(\frac{2}{\gamma+1}\right)^{1,4}\left(\frac{1}{M_\infty}\right)^{2,8}\left[\frac{2\gamma M_\infty^2 - (\gamma-1)}{\gamma+1}\right] - 1\right\}$$

For blunt-based bodies in supersonic flow, Gabeaud derived the equation for the base pressure coefficient, while the skin-friction contribution was computed using Van Driest II method [29] as suggested in Ref. [28]. Van Driest method can be thought of as a transformation method, relating the skin-friction coefficient to the Reynolds number. For most flows, a portion of the flow is laminar and an approximation to the mean skin-friction coefficient for laminar flow can be obtained from:

$$C_{SF} = 1.328/\sqrt{Re}$$

The mean turbulent skin-friction over the entire body or wing area, instead, is computed as [30]:

$$C_{SF} = C_{f\infty} * \frac{A_{wet}}{A_{ref}}$$

From the knowledge of the axial and normal coefficients, the computation of the lift and drag coefficients can be retrieved through the following equation.

$$C_L = C_N \cos\alpha - C_A \sin\alpha$$
$$C_D = C_N \sin\alpha + C_A \cos\alpha$$

3.2 Propulsion parameters estimation

In this section, the propulsion subsystem is discussed. As of the current date, it consists of the SRM model, but in the future, it could be expanded to include liquid or hybrid technologies. In the context of SRMs, grain design significantly influences parameters such as burning area, chamber pressure, net thrust profiles, volumetric efficiency, and geometric dimensions of the motor. However, designing grain shape is complex and involves numerous variables. To simplify the initial modelling step, a constant thrust profile was defined for Space Propulsion (SP) motors in launch vehicles. It represents neutral star grains with pressure variations below 15% of the nominal value. From CEA [31]- T_c, P_c, M_{mol}, c_p, I_{sp}, ε - are obtained.

The performance values are then analytically verified through the following equations:

$$C^* = \sqrt{\frac{T_c\, R}{M_{mol}\, k\, \left(\frac{2}{k+1}\right)^{\left(\frac{k+1}{k-1}\right)}}}$$

$$C_T = \sqrt{\frac{2k^2}{k-1}\left(\frac{2}{k+1}\right)^{\left(\frac{k+1}{k-1}\right)}\left[1 - \left(\frac{P_e}{P_c}\right)^{\left(\frac{k-1}{k}\right)}\right]} + \frac{(P_e - P_a)}{P_c}\varepsilon$$

$$I_{sp} = C^* C_T / g_0$$

Therefore, is was possible to obtain: $A_t = \frac{T}{P_c C_T}$ and $A_e = \epsilon A_t$, from which the exit diameter was also computed.

Knowing the mass flux, the propellant mass estimate is obtained:

$$\dot{m} = \frac{T}{C^* C_T}$$

$$I_{tot} = I_{sp}\, \dot{m}\, g_0\, t_b$$

$$m_{prop} = \dot{m}\, t_b * 1.02$$

The next step is to estimate the engine length required to contain the propellant, which depends on the selected grain geometry. Currently, the available option is a star-shaped grain, which ensures a constant thrust profile and can be modeled using a simplified approach. Future work

Copyright 2024 by Mr. Vassilios Silaidis. Published by the IAF, with permission and released to the IAF to publish in all forms .

will explore the potential extension of this geometry to other grain types

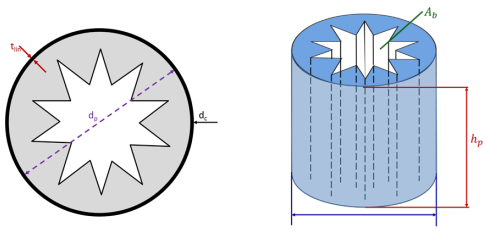

Figure 2: star grain propellant configuration

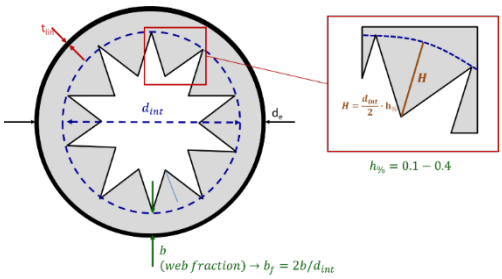

Figure 3: star grain parameters

Considering a burning rate $r_b = 1.2 * (P_c)^{0.41}$ (Note: Pc in [atm]), and knowing from the chosen propellant type, its density ρ, we can derive:

$$A_b = \frac{\dot{m}}{r_b \rho}, \qquad A_b^{in} = A_b^{end}$$

From which the engine length is derived: $h_p = \frac{A_b}{\pi d_p}$ - assuming a thickness of the structure t_{lin} and a diameter d_c, such that the internal grain diameter is $d_p = d_c - 2t_{lin}$. Finally, it is possible to estimate the number of wheat stars using the formula, knowing the star perimeter, where $h_{\%}$ is a value between 1 and 4.

$$P_{int} = \pi \cdot d_{bs} \cdot \sqrt{1 + \frac{N \cdot h_{\%}}{\pi}}$$

$$N_{punte} = \frac{\pi}{h_{\%}} \cdot \left[\left(\frac{P_{int}}{\pi \cdot d_{bs}}\right)^2 - 1\right]$$

3.3 Masses estimation

Once the geometrical details of the launcher and its components are defined, a preliminary mass estimation is performed using MERs derived from the literature [32].

4. Nominal case mission

For the simulation of this study-case a three stage, winged and rocket powered air-launched system has been chosen. These main characteristics are taken from the main air-launched flight proven system existent: Pegasus XL[5]. The detailed characteristics of the chosen baseline are resumed in Tables 1,2,3:

Table 1: baseline motor characteristics

Parameter	Units	Stage 1	Stage 2	Stage 3
Length	[m]	8.314	2.828	1.275
Diameter	[m]	1.35	1.35	0.95
Inert mass	[Kg]	2423	698	145
Propellant	[Kg]	17952	5171	1070
Burn time	[s]	68.5	69.7	66.8
Max Thrust	[kN]	715	200	40
Sp. Impulse	[s]	291	291	290

Table 2:baseline mass properites

Parameter	Mass [Kg]
Fairing	175
Wing	131
Payload	220
Avionics	75
Wiring	23.2
Propellant	24193
Engines Struc.	3265
GLOW	28084

Table 3: baseline external geometrical parameters

Parameter	Value	Units
l	16.25	[m]
d	1.35	[m]
l_w	8.12	[m]
l_t	14.75	[m]
l_n	2.7	[m]
$nose$	'E'	[-]
c_{rw}	3.3	[m]
b_w	6.5	[m]
c_{rt}	1.5	[m]
b_t	3.0	[m]
λ	30	[deg]

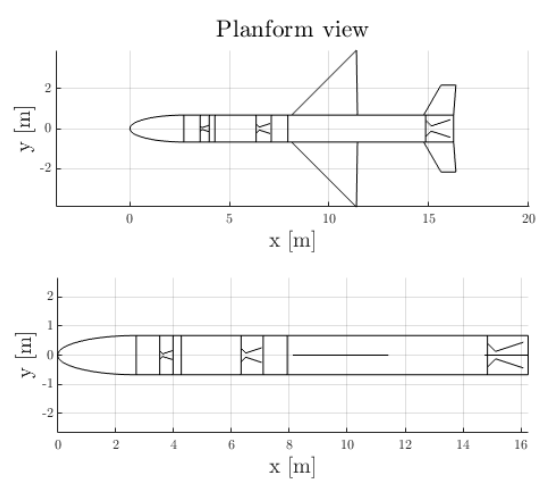

Figure 4: baseline representation (planform and side view)

Copyright 2024 by Mr. Vassilios Silaidis. Published by the IAF, with permission and released to the IAF to publish in all forms .

Giving all these inputs to the 3DOF simulator and specifying all the mission analysis data related to the ascent phase, it was possible to retrieve the nominal trajectory for this case-study.

5. Optimization Architecture, Inputs and Options

The general outline of the model architecture for the optimisation is shown in Appendix A.

Given the geometrical and propulsive input parameters, the aerodynamics and propulsion performances are evaluated. With this information, the geometry of the body can be defined, and an initial estimation of the mass is performed. Given also the trajectory control inputs, after an atmospheric and flight conditions prediction is possible to simulate the trajectory and thus final performance of the candidate through the integration of the equations of motion.

The architecture of the system allows the variables coming out the analysis of a subsystem to be given as input to the next one, and that the latter simultaneously influences the first according to the selected constraints.

Since the tool utilises a genetic algorithm optimiser, it offers robustness and is suitable for complex issues with multiple variables and can also achieve global convergence relying on statistical principles.

The control vector containing all the optimization variables is:

$$u_{control} = u_{propulsion} + u_{aerodynamics} + u_{trajectory}$$

The upper and lower boundary conditions for the research are given in Tables 4,5,6.

Table 4: $u_{aerodynamics}$ controls and boundaries

	LB	UB	UI
d	1.20	1.50	[m]
l_w	0.8	1.15	[-]
l_t	0.8	0.98	[-]
l_n	1.5*d	4*d	[m]
$nose$	0.5	3.5	[-]
c_{rw}	3	3.5	[m]
b_w	6.5	6.7	[m]
c_{rt}	1	2	[m]
b_t	2.5	3.5	[m]
λ	25	35	[deg]

Table 5: $u_{propulsion}$ controls and boundaries

	LB	UB	UI
T_1	700	730	[kN]
T_2	180	200	[kN]
T_3	35	40	[kN]
t_{b1}	65	70	[s]
t_{b2}	65	70	[s]
t_{b3}	65	70	[s]

Table 6: $u_{trajectory}$ controls and boundaries

	LB	UB	UI
$\theta_1(t)$	25	29	[deg]
$\theta_2(t)$	22	30	[deg]
$\theta_3(t)$	15	25	[deg]
$\theta_4(t)$	43	49	[deg]
$\theta_5(t)$	15	20	[deg]
$\theta_6(t)$	-2	5	[deg]
$\theta_7(t)$	-20	-25	[deg]
$\theta_8(t)$	10	20	[deg]
$\psi_1(t)$	-10	-15	[deg]
$\psi_2(t)$	-15	-20	[deg]
$\psi_3(t)$	-10	-15	[deg]
$\psi_4(t)$	0	5	[deg]
$\psi_5(t)$	0	5	[deg]
$\psi_6(t)$	0	5	[deg]
$\psi_7(t)$	-5	10	[deg]
$\psi_8(t)$	-5	10	[deg]

Where the navigation inputs $\theta(t)$ and $\psi(t)$, which are pitch and yaw angles in a Topocentric Horizon Frame, are converted to ECI frames and decomposed to get $\hat{u}(t)$.

Objective function and mission constraints

The fitness function can be written in such a way to consider several objectives simultaneously. This is possible if one uses an explicit expression given by the sum of several contributions that can be tuned by means of weights. The sum of the weights must be unitary - for computational reasons – and the contributions of the function are normalised so that those with higher numerical values are not given priority. The generalized equation is in the form of:

$$w_1 + w_2 + \cdots + w_n = 1$$

$$f_{W,N}(x) = w_1 \frac{f_1(x)}{f_1 *} + w_2 \frac{f_2(x)}{f_2 *} + \ldots + w_n \frac{f_n(x)}{f_n *}$$

Where $f_i(x)$ is the performance value to be minimized (or maximized). This approach using weights is not the only one in the literature, there are in fact more refined techniques capable of solving multi-objective problems, which exploit evolutionary algorithms (EMO), resulting in solutions in the so-called Pareto front [33].

However, for this specific problem, the function selected to be minimized was

$$f_{W,N}(x) = w_1 \frac{m_0}{m} - w_2 \frac{h_f}{h}$$

For the multidisciplinary study, 12 complementary numbers ranging from 0 to 1 were selected as weight values such that $w_1 = n$ and $w_2 = 1 - n$. A result was

Copyright 2024 by Mr. Vassilios Silaidis. Published by the IAF, with permission and released to the IAF to publish in all forms .

generated for each pair of weights and subsequently post-processed. The minimization of mass at take-off is a typical objective function for rocket design, since it is strictly related with engineering costs.
Regarding the genetic optimisation parameters, the following were selected in this example: number of candidates equal to 120, crossover fraction equal to 0.8, 10 elite candidates per generation and mutation possible. Finally, the constraints of the selected problem are 18:16 inequality and 2 equality constraints - and can be resumed by these 8 equations:

Table 7: constraints selected for optimization

No.	Constraint
(1)	$5 < \frac{l}{d} < 25$
(2)	$X_{static} < 0$
(3)	$1.5 < \frac{T_i}{W_i} < 5$
(4)	$7 < r_{b1} < 15$
(5)	$5 < r_{b23} < 15$
(6)	$e_f < 0.1$
(7)	$i_f = i_{sso}$
(8)	$\gamma_f = 0$

Constraint (1) is used to guarantee preliminary structural integrity of the system, (2) is for the static stability of the system before the first stage detachment (it ensure that the aerodynamic centre is behind the centre of mass), (3),(4) and (5) are feasibility checks about the propulsion, in particular to guarantee that the grain can be produced and that it will not burn to fast (or too slow). Finally (6) (7) and (8) are trajectory final constraints, particularly important for the orbit insertion: the final orbit must be nearly circular Sun-Synchronous.

6. Results

For each of the 12 GA runs, the initial population was randomly produced generating 120 candidates with values of the genes ranging inside the lower and upper boundaries imposed, a visual representation of the initial population is given in figure Appendix A.
Among the candidates generated for each of the pair of weights selected, the one that best met the desired conditions was chosen. The graph in Fig. 11 illustrates the values of the fitness function based on the selected pair of weights - also evaluating the maximum height reached and the initial mass of the chosen candidate.

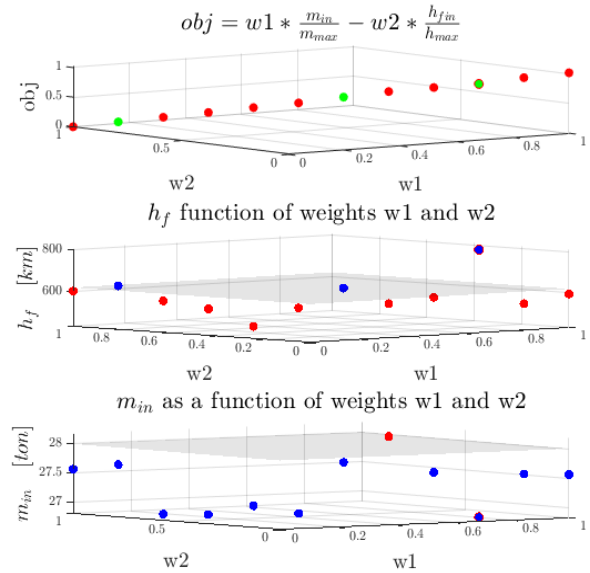

Figure 5: final optimal candidates generated as function of input weights, initial mass and final altitude reached. Blue dots have $m_0 < 28000kg$ or $h_f > 620km$

The blue dots in the altitude graph subplot represent configurations whose final height exceeds the height of 620 km, while the red dots indicate configurations that do not meet this criterion. Similarly, the blue dots in the mass subplot represent configurations with an initial mass less than 28,000 kg.
At the end of the optimization, only three final candidates (points highlighted in green) meet both requirements. Among these – one must be eliminated as it is not feasible with respect to the constraints imposed. The optimal candidate therefore is the one that corresponds to the pair of weights $w_1 = 0.182$ and $w_2 = 0.818$.
This configuration was selected for further study, and its results were post-processed accordingly. In the figure below, the overlap of the new candidate external geometry with respect to the starting baseline is shown.

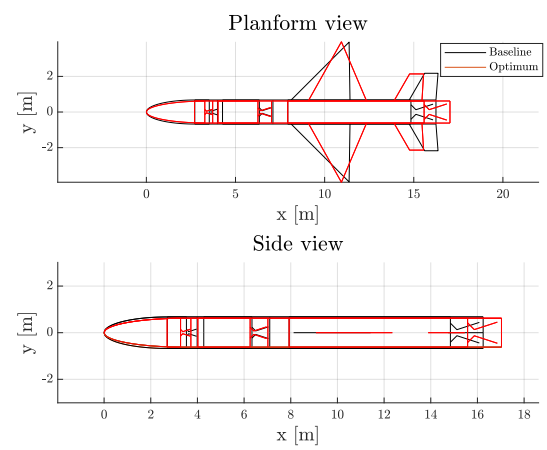

Figure 6: new configuration (red) vs baseline (black) external geometry

Copyright 2024 by Mr. Vassilios Silaidis. Published by the IAF, with permission and released to the IAF to publish in all forms .

The tables below show the new propulsion features and the new mass budget. What we can see is that the new engines have a lower overall thrust than those of the baseline, are longer and have a lower diameter. This, according to the design made, leads to a significant decrease in propellant mass. In addition, the new configuration has a wing with a smaller sweep angle and symmetrical geometry, and the tail wings are moved further forward.

Table 8: new configuration's propulsion characteristics

Parameter	Units	Stage 1	Stage 2	Stage 3
Length	[m]	9.1	3.0	1.01
Diameter	[m]	1.24	1.24	0.95
Inert mass	[Kg]	2477	691.5	139.4
Propellant	[Kg]	17615	5123	1033
Burn time	[s]	68.5	69.7	66.8
Max Thrust	[kN]	701	198	37.5
Sp. Impulse	[s]	291.2	291.1	290.8

Table 9: new configuration's mass properties

Parameter	Mass [Kg]
Fairing	125.9
Wing	130
Payload	220
Avionics	75
Wiring	24.35
Propellant	23771
Engine Struc.	3307
GLOW	27654

At the end of the optimisation all the required constraints were satisfied, while getting an objective function (i.e. mass at lift-off and final height) optimised.
The mass of the optimized configuration is 27654 kg, with respect to the initial configuration which had a mass of 28084 kg - the final height is of 627 km vs 629 of the baseline.

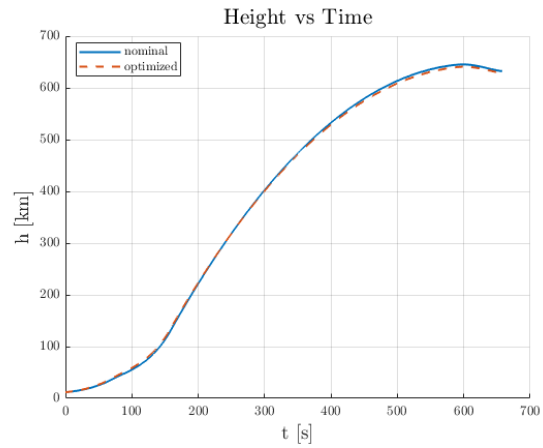

Figure 7: trajectory comparison: the new configuration reaches the orbital requirements, with a final mass reduced of 1.5%

5. Discussion

The presented optimization framework successfully generates final configurations consistent with the selected design boundaries across all weight series. However, approximately two-thirds of the resulting configurations fail to meet the mission requirements. This suggests that either the mission constraints must be relaxed, or the design boundaries expanded to allow for a larger search space and the generation of more viable candidates. Among the configurations, two meet all constraints and outperform the baseline in overall performance. The best configuration is selected based on the lowest liftoff weight, which is prioritized as the most critical parameter. It is therefore demonstrated how such a framework can be useful in the optimization of a multi-disciplinary mission that involves simultaneously aspects of aerodynamics, propulsion, mass sizing and navigation. Important aspects such as the choice of the objective function, the design boundaries and the selected mission constraints will be the subject of subsequent research, with the aim of understanding how and to what extent these parameters can influence the quality of the proposed optimal design.

6. Conclusions

The proposed MDO framework has been successfully tested and produces promising results. The launch vehicle produced by the optimization process can reach an orbit that satisfies all constraints (with a maximum height of less than 1% with respect to the baseline) but with an initial mass of the object 1.5% lower (430kg less than baseline), which is a promising result in term of cost reduction. Future tests will be conducted to further validate the proposed methodology, focusing on decreasing the uncertainty of the models used in the analysis of the subsystems, and in addition, new analyses will be added to expand the quality of the preliminary design

Copyright 2024 by Mr. Vassilios Silaidis. Published by the IAF, with permission and released to the IAF to publish in all forms .

Appendix A (Trajectory Comparison)

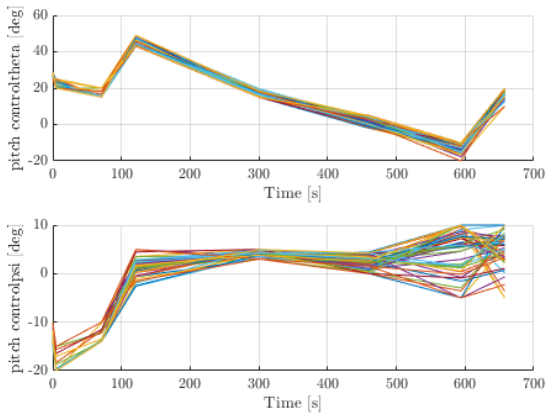

Figure 8: trajectory controls evaluated during a GA cycle

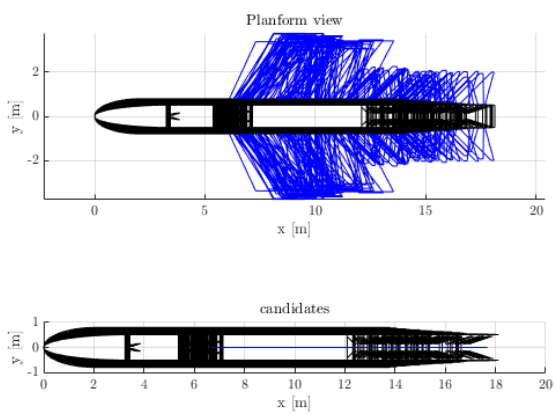

Figure 9: candidates evaluated during a GA cycle

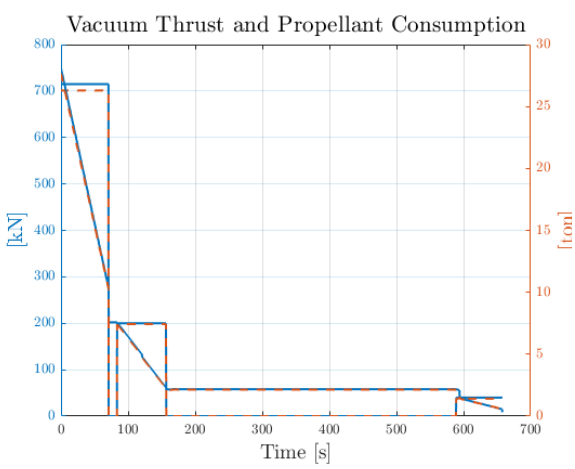

Figure 10: baseline(blue) vs new candidate (red dashed) thrust and mass data

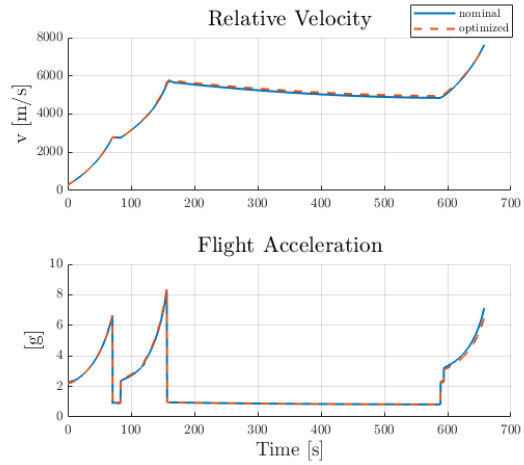

Figure 11: baseline(blue) vs new candidate (red dashed) trajectory data

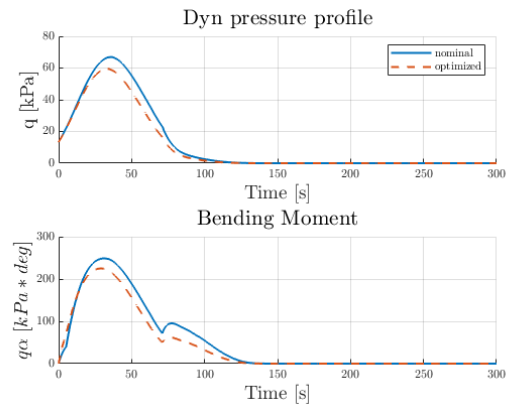

Figure 12:baseline(blue) vs new candidate (red dashed) trajectory data

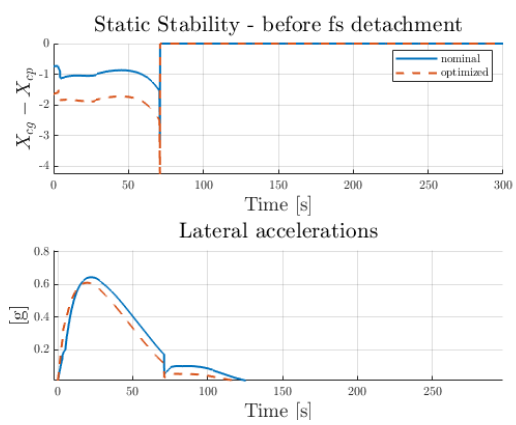

Figure 13:baseline(blue) vs new candidate (red dashed) trajectory data

Copyright 2024 by Mr. Vassilios Silaidis. Published by the IAF, with permission and released to the IAF to publish in all forms .

Appendix B (MDO framework)

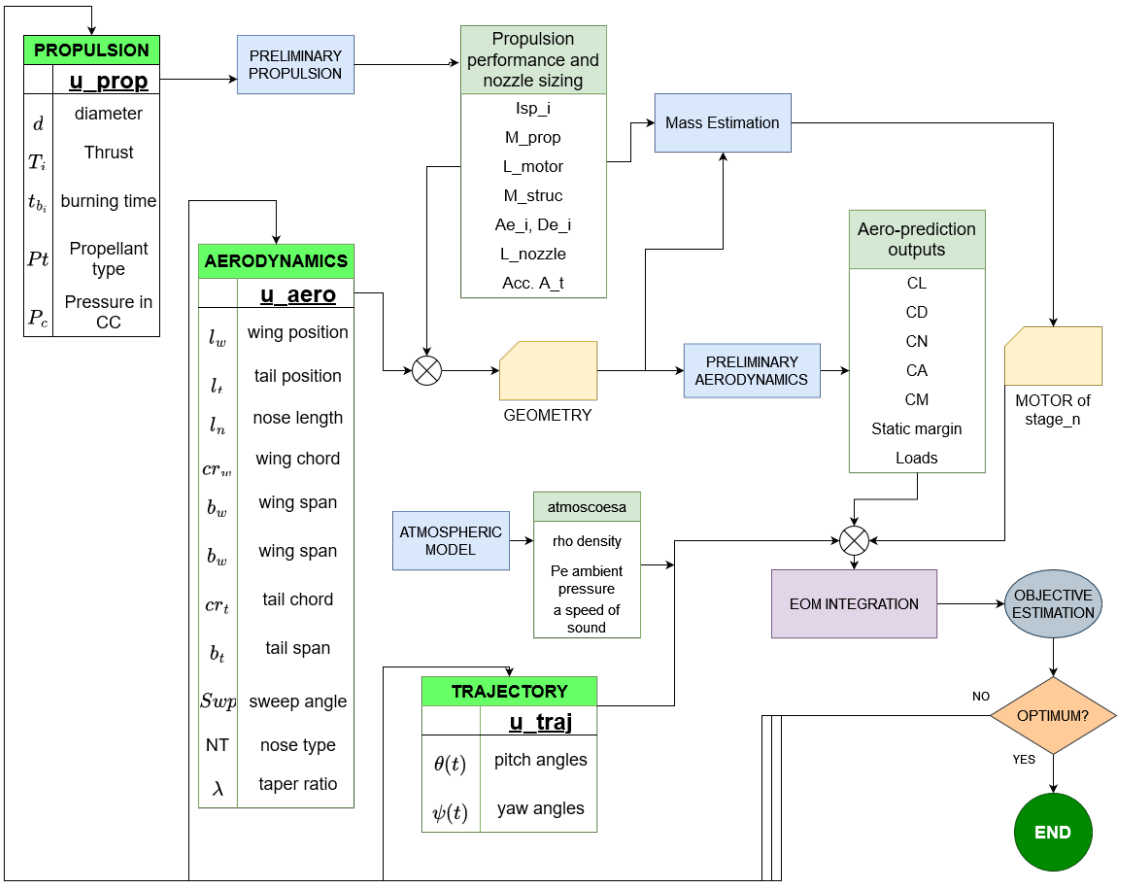

Figure 16: GA-MDO framework

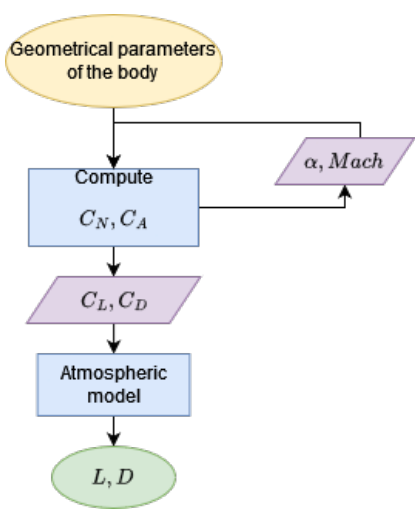

Figure 15: Aerodynamics estimation

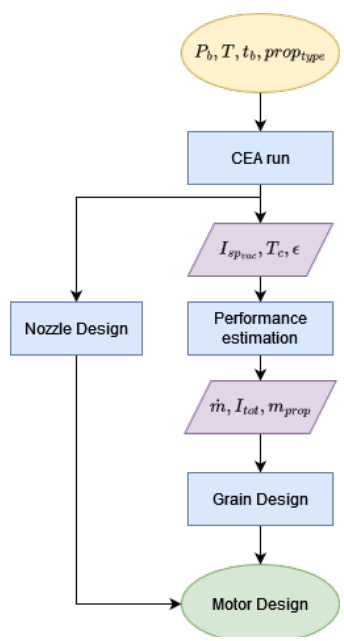

Figure 14: Motor design

Copyright 2024 by Mr. Vassilios Silaidis. Published by the IAF, with permission and released to the IAF to publish in all forms .

References

[1] "Satellite Industry Association," "State of the Satellite Industry Report," 2023.

[2] C. A. Maddock *et al.*, "Vehicle and mission design of a future small payload launcher," in *21st AIAA International Space Planes and Hypersonics Technologies Conference*, 2017.

[3] T. Wekerle, J. B. P. Filho, L. E. V. L. da Costa, and L. G. Trabasso, "Status and trends of smallsats and their launch vehicles - An up-to-date review," Jul. 2017, *Departamento de Ciencia e Tecnologia Aeroespacial, São José dos Campos*. doi: 10.5028/jatm.v9i3.853.

[4] Kulu Erik, "Small launchers-2021 industry survey and market analysis," *72nd International Astronautical Congress (IAC 2021), Dubai, United Arab Emirates,* 2021.

[5] "Northrop Grumman Corporation," "PegasusXL User Guide Release 8.2," Sep. 2020.

[6] Virgin Orbit, "Launcher One service guide," 2020.

[7] T. L. Holst, "Genetic Algorithms Applied to Multi-Objective Aerodynamic Shape Optimization," Moffett Field, California, Feb. 2005. [Online]. Available: http://www.sti.nasa.gov

[8] J. H. Holland, "Genetic Algorithms," *Sci Am*, vol. 267, no. 1, pp. 66–73, Jul. 1992, doi: 10.2307/24939139.

[9] R. I. Dancila and R. M. Botez, "New flight trajectory optimisation method using genetic algorithms," *Aeronautical Journal*, vol. 125, no. 1286, pp. 618–671, Apr. 2021, doi: 10.1017/aer.2020.138.

[10] R. Salvador, F. Patrón, A. Kessaci, and R. Mihaela Botez, "Flight trajectories optimization under the influence of winds using genetic algorithms," in *AIAA guidance, navigation, and control (GNC) conference*, Montreal, Quebec, Canada, 2013, p. 4620. [Online]. Available: www.larcase.etsmtl.ca

[11] M. Shafaee, P. Mohammadzadeh, A. Elkaie, and S. Abbasi, "Layout design optimization of a space propulsion system using hybrid optimization algorithm," *Proc Inst Mech Eng G J Aerosp Eng*, vol. 231, no. 2, pp. 338–349, Feb. 2017, doi: 10.1177/0954410016636914.

[12] D. B. Riddle, R. J. Hartfield, J. E. Burkhalter, and R. M. Jenkins, "Genetic-algorithm optimization of liquid-propellant missile systems," in *Journal of Spacecraft and Rockets*, American Institute of Aeronautics and Astronautics Inc., 2009, pp. 151–159. doi: 10.2514/1.30891.

[13] R. J. Hartfield, R. M. Jenkins, and J. E. Burkhalter, "Optimizing a solid rocket motor boosted ramjet powered missile using a genetic algorithm," *Appl Math Comput*, vol. 181, no. 2, pp. 1720–1736, Oct. 2006, doi: 10.1016/j.amc.2006.03.028.

[14] M. Fatehi and S. M. Hadi Taherzadeh, "Designing Space Cold Gas Propulsion System using Three Methods: Genetic Algorithms, Simulated Annealing and Particle Swarm," *Int J Comput Appl*, vol. 118, no. 22, pp. 975–8887, May 2015.

[15] M. B. Anderson and G. A. Gebert, "Using pareto genetic algorithms for preliminary subsonic wing design," in *6th Symposium on Multidisciplinary Analysis and Optimization*, American Institute of Aeronautics and Astronautics Inc, AIAA, 1996, pp. 363–371. doi: 10.2514/6.1996-4023.

[16] R. E. Perez, J. Chung, and K. Behdinan, "Aircraft conceptual design using genetic algorithms," in *8th Symposium on Multidisciplinary Analysis and Optimization*, 2000. doi: 10.2514/6.2000-4938.

[17] M. B. Anderson, J. E. Burkhalter, and R. M. Jenkins, "Design of a guided missile interceptor using a genetic algorithm," *J Spacecr Rockets*, vol. 38, no. 1, pp. 28–35, 2001, doi: 10.2514/2.3668.

[18] M. B. Anderson, J. E. Burkhalter, and R. M. Jenkins, "Missile aerodynamic shape optimization using genetic algorithms," *J Spacecr Rockets*, vol. 37, no. 5, pp. 663–669, 2000, doi: 10.2514/2.3615.

[19] D. J. Bayley, R. J. Hartfield, J. E. Burkhalter, and R. M. Jenkins, "Design optimization of a space launch vehicle using a genetic algorithm," *J Spacecr Rockets*, vol. 45, no. 4, pp. 733–740, 2008, doi: 10.2514/1.35318.

[20] W. A. Crossley, "Optimization for Aerospace Conceptual Design through the use of Genetic Algorithms," in *Proceedings of the First NASA/DoD Workshop on Evolvable Hardware*, 1282 Grissom Hall, West Lafayette, IN: IEEE, 1999.

[21] L. Blasi, L. Iuspa, and G. Del Core, "Conceptual aircraft design based on a multiconstraint genetic optimizer," *J Aircr*, vol. 37, no. 2, pp. 351–354, 2000, doi: 10.2514/2.2604.

[22] M. B. Anderson, "Genetic Algorithms In Aerospace Design: Substantial Progress, Tremendous Potential," in *Brussels: NATO/Von Karmen Institute Workshop on Intelligent System*, 2002, pp. 13–17.

[23] G. Di Campli, B. De Volo, M. Naeije, C. Roux, and M. Volpi, "Vega Launchers' Trajectory Optimization Using a Pseudospectral Transcription," in *8th European Conference for*

Copyright 2024 by Mr. Vassilios Silaidis. Published by the IAF, with permission and released to the IAF to publish in all forms .

Aeronautics and Aerospace Sciences, 2019. doi: 10.13009/EUCASS2019-710.

[24] E. C. Coşkun, "Multistage launch vehicle design with thrust profile and trajectory optimization," Middle East Technical University, 2014.

[25] L. H. Jorgensen, "Prediction of static aerodynamic characteristics for slender bodies alone and with lifting surfaces to very high angles of attack," Washington, No. NASA-TR-R-474, 1977.

[26] L. H. Jorgensen, "Prediction of static aerodynamic characteristic for space-shuttle-like and other bodies at angles of attack from 0° to 180°," No. NASA-TN-D-6996, 1973.

[27] W. C. Pitts, J. N. Nielsen, and G. E. Kaattari, "Lift and center of pressure of wing-body-tail combinations at subsonic, transonic and supersonic speeds," No. NACA-TR-1307, 1959.

[28] L. H. Jorgensen, "A method for estimating static aerodynamic characteristics for slender bodies of circular and noncircular cross section surfaces at angles of attack from 0° to 90°," No. A-4700, 1973.

[29] E. J. Hopkins, "Charts for predicting turbulent skin friction from the Van Driest method," Moffett Field, California, 1972.

[30] AGARD, "Special Course on Missile Aerodynamics," Neuilly Sur Seine,France, Jun. 1994.

[31] I. Analysis, S. Gordon, A. Cleveland, and B. J. Mcbride, "NASA Reference Computer Program for Calculation Complex Chemical Equilibrium Compositions and Applications," No. NAS 1.61: 1311, 1994.

[32] Don Edberg and Willie Costa, "Design of Rockets and Space Launch Vehicles Second Edition," Reston, Virginia, 2022.

[33] K. Deb, "Multiobjective Optimization Using Evolutionary Algorithms Multi-Objective Optimization Using Evolutionary Algorithms: An Introduction," *Springer London*, pp. 3-34., Feb. 2011, [Online]. Available: http://www.iitk.ac.in/kangal/deb.htm